

Optimal Control of Endemic Epidemic Diseases With Behavioral Response

Original

Optimal Control of Endemic Epidemic Diseases With Behavioral Response / Parino, F., Zino, L., Rizzo, A.. - In: IEEE OPEN JOURNAL OF CONTROL SYSTEMS. - ISSN 2694-085X. - ELETTRONICO. - 3:(2024), pp. 483-496.
[10.1109/ojcsys.2024.3488567]

Availability:

This version is available at: 11583/2994007 since: 2024-11-23T18:06:42Z

Publisher:

IEEE

Published

DOI:10.1109/ojcsys.2024.3488567

Terms of use:

This article is made available under terms and conditions as specified in the corresponding bibliographic description in the repository

Publisher copyright

(Article begins on next page)

Optimal control of endemic epidemic diseases with behavioral response

FRANCESCO PARINO^{1§}, LORENZO ZINO¹ (Senior Member, IEEE),
ALESSANDRO RIZZO^{1,2} (Senior Member, IEEE)

¹Department of Electronics and Telecommunications, Politecnico di Torino, 101029 Torino, Italy

CORRESPONDING AUTHOR: A. Rizzo (e-mail: alessandro.rizzo@polito.it)

ABSTRACT Behavioral factors play a crucial role in the emergence, spread, and containment of human diseases, significantly influencing the effectiveness of intervention measures. However, the integration of such factors into epidemic models is still limited, hindering the possibility of understanding how to optimally design interventions to mitigate epidemic outbreaks in real life. This paper aims to fill in this gap. In particular, we propose a parsimonious model that couples an epidemic compartmental model with a population game that captures the behavioral response, obtaining a nonlinear system of ordinary differential equations. Grounded on prevalence-elastic behavior—the empirically proven assumption that the disease prevalence affects the adherence to self-protective behavior—we consider a nontrivial negative feedback between contagions and adoption of self-protective behavior. We characterize the asymptotic behavior of the system, establishing conditions under which the disease is quickly eradicated or a global convergence to an endemic equilibrium is attained. In addition, we elucidate how the behavioral response affects the endemic equilibrium. Then, we formulate and solve an optimal control problem to plan cost-effective interventions for the model, accounting for their healthcare and social-economical implications. Numerical simulations on a case study calibrated on sexually transmitted diseases demonstrate and validate our findings.

INDEX TERMS epidemics, nonlinear control systems, optimal control, game-theory

I. INTRODUCTION

The spread of epidemic diseases has always been one of the most severe threats to mankind. Hence, the design of efficient plans and interventions for the containment of epidemic diseases is a task of paramount importance in our societies. However, designing such plans is extremely challenging from several perspectives, ranging from healthcare to the social and economic impact of the interventions. In particular, in most cases, only a set limited amount of resources is available to plan interventions. Hence, the study and design of optimal policies is a crucial aspect. In recent decades, the development of mathematical models of epidemic spreading has provided new tools to predict the evolution of epidemic outbreaks and test what / if scenarios [1]–[5]. In particular, the growing interest in epidemic modeling within the systems and controls community has triggered the development of novel model-informed control strategies [6]–[17], to help assist public health authorities in their complex decisions concerning the planning of intervention policies.

Recent epidemic outbreaks, such as Ebola in West Africa and the global COVID-19 pandemic, have highlighted human behavior and individual responses as fundamental factors in shaping the course of an outbreak. Understanding human behavior is also crucial for designing effective strategies to control infectious diseases [18]. In fact, especially when pharmaceutical interventions and treatments are insufficient or impractical, the collective adoption of self-protective behaviors becomes essential for controlling outbreaks [19].

In this context, there is an urgent need for epidemic models that integrate social and behavioral dynamics, capturing the complex interplay between disease evolution and population behavior [19]. In recent years, the integration of behavioral responses into mathematical models for epidemics has gained considerable attraction within the scientific community [20], [21], addressing the issue from various perspectives. Awareness-based models examine the spread of the disease in conjunction with information and concern about it [22]–[25]. Other approaches explicitly model human behavior through additional states [26], or use co-evolving dynamics based on opinion dynamics [27]. Game-theoretic frameworks consider factors like social influence, perceived

[§]Current address: Sorbonne Université, INSERM, Pierre Louis Institute of Epidemiology and Public Health (IPLESP), 75013 Paris, France

infection risk, accumulating fatigue, social and economic costs, bounded rationality, and government-mandated interventions [28]–[33]. Based on these approaches, some control methods have been developed to design intervention policies with the final goal of reducing the number of infections [34], [35]. Despite these efforts, many key questions related to the control of such mathematical frameworks remain mostly unexplored, in particular concerning the design of intervention policies that seek to optimize both the healthcare and social-economical impact of the control.

Here, our objective is to advance the growing body of research in epidemic–behavioral models [28]–[35], by providing insights into optimal control policies for these types of models. Given the limited knowledge and lack of consensus on the mechanisms governing human behavior, we develop a parsimonious, yet general, model that captures the feedback loop between the disease spreading and individual choices. In particular, we pair a susceptible–infected–susceptible (SIS) compartmental epidemic model [3] with a game-theoretic mechanism [36]. The former emulates the diffusion of the pathogen within the population, while the latter captures the behavioral responses to the spreading of the epidemic.

The game-theoretic approach effectively captures the complexity of collective human behavior considering that individuals make decisions to maximize their utility function. We based such a utility function on the idea of “prevalence elastic behavior” [37], where disease prevalence influences adherence to self-protective behavior. Simply put, higher infection rates make self-protection more appealing, while lower rates reduce the incentive. For instance, during the AIDS outbreak in the US, an increased demand for condoms was registered [38]. The coupling between epidemic and behavioral creates a feedback between contagion and adoption of self-protective behavior. This feedback can make the implementation of policies nontrivial: favoring the adoption of self-protective behavior leads to less new infections, which, in turn, decreases the incentives for adopting self-protective behavior, increasing new infections.

Technically, we formulate the model as a planar system of coupled nonlinear ordinary differential equations (ODEs). Then, our main contribution is threefold. First, through the analysis of such a system, we characterize its asymptotic behavior. In particular, we establish an epidemic threshold: if the contagion rate is below such a threshold, the system converges to a disease-free equilibrium, i.e., the epidemic disease is quickly eradicated. Above such a threshold, the system converges to an endemic equilibrium. Different endemic equilibria are possible, and the model parameters determine which of these is globally asymptotically stable. Second, we incorporate in the model an explicit control action in terms of an input that represents the incentives (or disincentives) implemented by public health authorities to favor the adoption of self-protective behavior. For instance, for STIs, such a term can capture free condom distributions [39] or the implementation of awareness campaigns [40]. We use

the model to design the control input to optimally trade-off between the healthcare impact of the disease and the social and economical impact of the interventions while steering the system to a desired state. We establish a method to design such an optimal policy by leveraging the Pontryagin’s Maximum Principle [41], [42]. Third, using the developed framework, we validate our approach in a case study inspired by the spread of sexually transmitted infections (STIs). In summary, our method provide novel control-theoretic insight into the spread of epidemic disease and the possibility to steer a population’s behavioral response to mitigate the outbreak. In particular it demonstrates that, even in parsimonious models, nontrivial strategies may emerge as optimal, when considering the interdependence between epidemic spreading and human behavioral response.

We organize the rest of the article as follows. Section II introduces the epidemic–behavioral model, which is studied in Section III. In Section IV, we formulate and analyze the optimal control of the model. In Section V, we discuss a case study on STIs. Section VI concludes the paper and outlines avenues for future research.

II. MODEL

We consider the spread of an infectious disease in a population of constant size. At each time $t \geq 0$, the state of the population is described by the fraction of infected individuals, denoted by $I(t) \in [0, 1]$, and the fraction of individuals who adopt self-protective behavior, denoted by $P(t) \in [0, 1]$ — the fractions of susceptible individuals and individuals who do not adopt self-protective behavior are equal to $1 - I(t)$ and $1 - P(t)$, respectively. We define an epidemic–behavioral model by coupling the dynamics of the two state variables $I(t)$ and $P(t)$. Specifically, the adoption of self-protective behavior influences the disease progression by affecting the infection rate; while, following the assumption of prevalence-elastic behavior [37], the adoption of self-protective behavior depends on the fraction of infected individuals.

A. EPIDEMIC DYNAMICS

We build our dynamics on a deterministic population SIS model [3], which describes the evolution of the fraction of infected individuals $I(t)$ as governed by the following ODE:

$$\dot{I} = \delta(1 - I)I - \gamma I, \quad (1)$$

where $\delta \geq 0$ is the *infection rate* and $\gamma > 0$ is the *recovery rate*. Briefly, the rate of change of the fraction of infected individuals in Eq. (1) comprises two terms. The first one is a positive contribution that accounts for new infections and is proportional to the infection rate δ and to the interaction rate between susceptible individuals and infected ones, which is given by the product $(1 - I)I$. The second term, which accounts for recovered individuals, is negative and is proportional to the fraction of infected individuals who recover, according to the recovery rate. More details of the formulation of the SIS model can be found in recent survey papers [3], [5]. Without any loss in

generality, we can re-scale the time variable to set $\gamma = 1$, thus reducing the parameters of the epidemic model to just the (normalized) infection rate $\beta > 0$ (obtained as $\beta = \delta/\gamma$), which coincides with the well-known concept of the *basic reproduction number* of the disease [5].

We model the adoption of self-protective behavior through a modification of the infection rate. Hence, we rewrite β as a time-varying function that depends on time through the fraction of adopters of self-protective behavior, i.e., $\beta(t) = \beta(P(t))$, obtaining the following dynamics:

$$\dot{I} = \beta(P)(1 - I)I - \gamma I. \quad (2)$$

B. BEHAVIORAL DYNAMICS

We formulate the individuals' choice on whether to adopt self-protective behavior or not as a *population game* [36]. Such a game is characterized by two strategies, $\mathcal{S} = \{p, u\}$, where p and u represent the choice of adopting self-protective behavior and not adopting them, respectively.

Each strategy is associated with a utility function $\pi_p(t)$ and $\pi_u(t)$, respectively, which represents the reward that a generic individual would receive by choosing strategy p or u at time t , respectively. Here, we assume that these utility functions depend on the current number of infected individuals in the population, i.e., $\pi_p(t) = \pi_p(I(t))$ and $\pi_u(t) = \pi_u(I(t))$. Note that, unlike classical population games, here we are assuming that the utility functions depend on the state of the population through an external variable ($I(t)$), rather than through the behavioral variable $P(t)$.

As time unfolds, individuals have the opportunity to revise their strategies to adhere to more successful ones implemented by some of their peers. Notably, each individual compares their utility functions with the one of other individuals, selected uniformly at random within the population. If the randomly selected individual has a higher utility, the individual switches to the superior strategy with probability proportional to the difference between the two utility functions. This revision protocol is usually referred to as *pairwise proportional imitation* [36], [43].

For large-scale populations, such an individual-level revision protocol can be captured by letting the overall rate at which individuals change their strategy from u to p to be proportional to the product of i) the fraction of adopters of u , ii) the fraction of adopters of p , and iii) the positive part of the difference between the two utility functions, i.e., $\max\{\pi_p - \pi_u, 0\}$. Similar, the overall rate of strategy change from p to u is proportional to the product of p , u , and the positive part of the opposite difference between the two utility functions, i.e., $\max\{\pi_u - \pi_p, 0\}$. Assuming that the revision process occurs at a constant rate $\varepsilon > 0$, which captures the relative velocity of the behavioral evolution with respect to the epidemic spreading, then through a mean-field approximation we obtain the well-known *replicator equation* [36], which can be written as the following ODE:

$$\dot{P} = \varepsilon(\pi_p(I) - \pi_u(I))P(1 - P) = \varepsilon\alpha(I)P(1 - P), \quad (3)$$

where we denote $\alpha(I) := \pi_p(I) - \pi_u(I)$ as the difference between the two utility functions associated with strategy u and p , which captures the advantage that an individual perceives for adopting self-protections when the fraction of infected population is equal to I . We term such a function as the *perceived advantage of self-protective behavior*.

Remark 1. *In this model, the behavior of individuals is not affected by their health state. This assumption is reasonable for many endemic infectious diseases such as many STIs, where infected individuals are actually unaware of being infected for most of the time of infection, and as soon as they get aware of their health status, the recovery is extremely fast compared to the time needed to discover the disease. For this reason, we can assume that infected individuals and susceptible individuals have the same behavior.*

C. COUPLED EPIDEMIC-BEHAVIORAL SYSTEM

By coupling the epidemic dynamics in Eq. (2) and the behavioral dynamics in Eq. (3), we obtain the following planar system of autonomous nonlinear ODEs:

$$\begin{cases} \dot{I} = \beta(P)(1 - I)I - I \\ \dot{P} = \varepsilon\alpha(I)P(1 - P). \end{cases} \quad (4)$$

As stated in the introduction, the most interesting and realistic setting contemplates the coupling of the disease and behavioral dynamics through a negative feedback, whereby $\beta(P)$ is a decreasing function of P and $\alpha(I)$ is an increasing function of I . Before discussing this assumption in detail (in the next section), we conclude this section by presenting an explanatory example of the coupled dynamical system.

Example 1 (Linear scenario). *Linear functions are an easy choice for setting $\alpha(I)$ and $\beta(P)$. In fact, in many scenarios it is plausible to assume that self-protective behavior reduce the probability of contracting the disease for those who adopt them. Let $\beta_0 \geq 0$ be the basic reproduction number of the disease (i.e the infection rate in the absence of self-protective behavior), and $a \in [0, 1]$ the efficacy of self-protective behavior, we can write the infection rate at the population level as a linear combination of β_0 and $a\beta_0$, respectively weighted by the fraction of population that does not adopt self-protective behavior and the fraction that does not make such an adoption, obtaining the following linear expression for the infection rate:*

$$\beta(P) = \beta_0((1 - P) + (1 - a)P). \quad (5)$$

Similarly, one can hypothesize that the utility function associated with the adoption of self-protective behavior ($u_p(I)$) increases linearly with the number of infected individuals as a response to an increasing concern about the epidemic spreading, according to a prevalence elastic behavior [37]. This has been observed, e.g., in the context of measles vaccination [44]. We can adopt a proportionality coefficient $w \geq 0$ that captures the reactivity of the population's behavioral response. The utility function associated with a lack of adoption of self-protective behavior remains constant and

equal to $c > 0$. This captures, e.g., the costs associated with the adoption of self-protective behavior (e.g., the economic costs of medical devices). Hence, we obtain

$$\pi_p = wI, \quad \pi_u = c, \quad \alpha(I) = wI - c. \quad (6)$$

that is, the difference in the utility functions $\alpha(I)$ increases linearly with the number of infected individuals as a response to increasing concern about the epidemic spreading.

Combining Eq. (6) and Eq. (5), the dynamical system with linear infection rate and perceived advantage of self-protective behavior takes the form:

$$\begin{cases} \dot{I} = \beta_0((1-P) + (1-a)P)(1-I)I - I \\ \dot{P} = \tilde{\varepsilon}(I-d)P(1-P), \end{cases} \quad (7)$$

where without any loss in generality, we have re-scaled the parameters in the second equation by introducing a parameter $d = c/w$ that captures the “difficulty” in adopting self-protective behavior as a trade-off between costs and perceived risks, and re-scaling $\tilde{\varepsilon} = w\varepsilon$.

III. ANALYSIS

We analyze the general dynamical system described in Eq. (4), focusing on the realistic scenario of a negative feedback described in the previous section. However, before making this assumption, we will first present some general properties of the coupled systems, which hold for any choice of the functions α and β that satisfies some minimal regularity assumptions, summarized in the following.

Assumption 1. *The functions α and β are continuously differentiable in $[0, 1]$ and take real and nonnegative real values, respectively, i.e., $\alpha : \mathcal{C}^1([0, 1]) \rightarrow \mathbb{R}$ and $\beta : \mathcal{C}^1([0, 1]) \rightarrow \mathbb{R}^+$.*

Under this regularity assumption, we prove that the coupled system is biologically well-posed, i.e., that the trajectories of the system are confined in the region $[0, 1] \times [0, 1]$. Moreover, we rule out the existence of limit cycles. These results are formally summarized in the following lemmas.

Lemma 1. *The domain $[0, 1] \times [0, 1]$ is positively invariant for Eq. (4) under Assumption 1.*

Proof: The domain $[0, 1] \times [0, 1]$ is compact and convex and the vector field in Eq. (4) is Lipschitz-continuous, since both $\alpha(I)$ and $\beta(P)$ are continuously differentiable functions. Hence, Nagumo’s Theorem can be applied [45]. We need to ascertain the direction of the vector field at the boundaries of the domain. We observe that $\dot{P} = 0$ for $P = 0$ and $P = 1$, while $\dot{I} = 0$ for $I = 0$ and $\dot{I} = -1$ for $I = 1$. This imply that any trajectory such that $(P(0), I(0)) \in [0, 1] \times [0, 1]$ has $(P(t), I(t)) \in [0, 1] \times [0, 1]$ for any $t \geq 0$. ■

Lemma 2. *Under Assumption 1, the system in Eq. (4) does not admit any nonconstant periodic solutions in $[0, 1] \times [0, 1]$.*

Proof: Using the Bendixson–Dulac criterion [46], we introduce the differentiable Dulac function $\varphi(I, P) =$

$\frac{1}{I(1-I)P(1-P)}$, and we verify that

$$\frac{\partial(\varphi\dot{I})}{\partial I} + \frac{\partial(\varphi\dot{P})}{\partial P} = -\frac{1}{(1-I)^2(1-P)P} + 0 \neq 0 \quad (8)$$

almost everywhere in the domain $[0, 1] \times [0, 1]$. Hence, by the Bendixson–Dulac criterion, we conclude that there is no closed orbit for the system in Eq. (4). ■

In the rest of this section, we study the equilibrium points of Eq. (4) and derive a global convergence result for the coupled system. As previously stated, we focus on a realistic scenario by making some assumptions on the perceived advantage of self-protective behavior $\alpha(I)$ and on the infection rate $\beta(P)$. In particular, we will assume that $\alpha(I)$ is an increasing function of the fraction of infected individuals, reflecting the fact that an increase in the number of infected makes more appealing to adopt self-protective behavior. We will further enforce that not to adopt self-protective behavior is the preferred strategy in the absence of any disease, while the adoption is felt as advantageous when the entire population is infected. Finally, we will assume that the infection rate $\beta(P)$ is a decreasing function of the fraction of individuals who use self-protective behavior P , which intuitively captures the effectiveness in adopting self-protections in preventing contagion. We formally summarize these conditions in the following assumption, which is stricter than Assumption 1.

Assumption 2. *The function $\alpha : \mathcal{C}^1([0, 1]) \rightarrow \mathbb{R}$ is such that $\alpha'(I) > 0$ for all $I \in [0, 1]$, $\alpha(0) < 0$, and $\alpha(1) > 0$. The function $\beta : \mathcal{C}^1([0, 1]) \rightarrow \mathbb{R}^+$ is such that $\beta'(P) < 0$ for all $P \in [0, 1]$.*

Under these assumptions, we can perform a complete analysis of the system. We start with a classification of all the equilibria of the coupled system and their local stability. To present our results, we first introduce some notation.

Definition 1. *Given an equilibrium point of Eq. (4) $\mathbf{x}^* = (I^*, P^*)$, we say that \mathbf{x}^* is a disease-free equilibrium (DFE) if $I^* = 0$; otherwise, if $I^* > 0$, we refer to it as an endemic equilibrium (EE).*

The classification of all the equilibria of Eq. (4) is summarized in the following statement.

Proposition 1. *Under Assumption 2, the system in Eq. (4) has at most five equilibria, denoted as $\mathbf{x}^{(i)} = (I^{(i)}, P^{(i)})$, $i \in \{1, 2, 3, 4, 5\}$. Specifically,*

- 1) $\mathbf{x}^{(1)} = (0, 0)$, which is a DFE with no adoption of self-protective behavior. This equilibrium is (locally) stable if $\beta(0) < 1$ and an (unstable) saddle point if $\beta(0) > 1$.
- 2) $\mathbf{x}^{(2)} = (0, 1)$, which is a DFE where the entire population adopts self-protective behavior. This equilibrium is always unstable (it is a saddle point if $\beta(1) < 1$ or a fully unstable point if $\beta(1) > 1$).
- 3) $\mathbf{x}^{(3)} = (1 - \frac{1}{\beta(0)}, 0)$, which is an EE with no adoption of self-protective behavior. This equilibrium exists if and

only if (iff) $\beta(0) > 1$; it is stable if $\beta(0) < (1 - \alpha^{-1}(0))^{-1}$ and a saddle point otherwise.

- 4) $\mathbf{x}^{(4)} = (1 - \frac{1}{\beta(1)}, 1)$, which is an EE where the entire population adopts self-protective behavior. This equilibrium exists iff $\beta(1) > 1$; it is stable if $\beta(1) > (1 - \alpha^{-1}(0))^{-1}$, and a saddle point otherwise.
- 5) $\mathbf{x}^{(5)} = (\alpha^{-1}(0), \beta^{-1}(\frac{1}{1 - \alpha^{-1}(0)}))$, which is an EE with partial adoption of self-protective behavior. This equilibrium exists if $\beta(1) < (1 - \alpha^{-1}(0))^{-1} < \beta(0)$; when it exists, it is always stable.

Proof: We compute the equilibria by setting the two ODEs in Eq. (4) to zero. From the first equation in Eq. (4), we obtain that the equation is equal to zero if either $I = 0$ or $\beta(P)(1 - I) = 1$. Imposing $I = 0$ in the second equation of Eq. (4), since $\alpha(0) < 0$, we observe that the equation is equal to zero iff either $P = 0$ or $P = 1$, yielding the equilibria $\mathbf{x}^{(1)}$ and $\mathbf{x}^{(2)}$. To study their stability, we compute the Jacobian matrix at a generic point, obtaining

$$J_h(I, P) = \begin{bmatrix} \beta(P)(1 - 2I) - 1 & \beta'(P)I(1 - I) \\ \varepsilon\alpha'(I)P(1 - P) & \varepsilon\alpha(I)(1 - 2P) \end{bmatrix}. \quad (9)$$

In $\mathbf{x}^{(1)}$, Eq. (9) reduces to a diagonal matrix with eigenvalues $\alpha(0) < 0$ and $\beta(0) - 1$, which yields stability condition $\beta(0) < 1$. In $\mathbf{x}^{(2)}$, the Jacobian matrix in Eq. (9) reduces to a diagonal matrix with eigenvalues $-\alpha(0) > 0$ and $\beta(1) - 1$. Hence, the equilibrium is always unstable.

We now look for equilibria with $I > 0$. The second equation in Eq. (4) is equal to zero if one of the following conditions is verified: 1) $P = 0$, 2) $P = 1$, or 3) $\alpha(I) = 0$.

- 1) For $P = 0$, from the condition for the first equation, $\beta(P)(1 - I) = 1$, we obtain $\beta(0)(1 - I) = 1$, i.e., $I = 1 - \frac{1}{\beta(0)}$, yielding equilibrium $\mathbf{x}^{(3)}$. Such a point belongs to the domain iff $\beta(0) > 1$. From Eq. (9), we observe that the Jacobian of the system evaluated in the equilibrium point has a negative eigenvalue equal to $1 - \beta(0)$, and an eigenvalue equal to $\varepsilon\alpha(1 - \frac{1}{\beta(0)})$, which is negative iff $\beta(0) < (1 - \alpha^{-1}(0))^{-1}$.
- 2) For $P = 1$, from the condition for the first equation, $\beta(P)(1 - I) = 1$, we obtain $\beta(1)(1 - I) = 1$, i.e., $I = 1 - \frac{1}{\beta(1)}$, yielding equilibrium $\mathbf{x}^{(4)}$. Such a point belongs to the domain iff $\beta(1) > 1$. From Eq. (9), we observe that the Jacobian of the system evaluated at the equilibrium has a negative eigenvalue equal to $1 - \beta(1)$ and an eigenvalue equal to $-\varepsilon\alpha(1 - \frac{1}{\beta(1)})$, which is negative iff $\beta(1) > (1 - \alpha^{-1}(0))^{-1}$.
- 3) From the condition $\alpha(I) = 0$, we obtain the condition $I = \alpha^{-1}(0)$, which exists and is unique due to Assumption 2. By plugging this condition in the first equation, we obtain $\beta(P)(1 - \alpha^{-1}(0)) = 1$, which yields the condition $P = \beta^{-1}(1/(1 - \alpha^{-1}(0)))$. Notice that such a condition can be satisfied by $P \in (0, 1)$ iff $\beta(1) < (1 - \alpha^{-1}(0))^{-1} < \beta(0)$. This equilibrium point coincides with $\mathbf{x}^{(5)}$. We can check that, such an

equilibrium exists, then it is always stable. In fact, from Eq. (9), we observe that the product of the off-diagonal terms is always negative, due to the properties of α' and β' . Hence, the eigenvalue equation for the Jacobian evaluated in $\mathbf{x}^{(5)}$ reduces to

$$\lambda \left(\lambda + \frac{\alpha^{-1}(0)}{1 - \alpha^{-1}(0)} \right) = -A, \quad (10)$$

where A is a strictly positive quantity, equal to the product of the off-diagonal terms of Eq. (9), with a negative sign. It is straightforward to observe that the solutions of Eq. (10), and thus the eigenvalues of the Jacobian evaluated in the equilibrium point, are necessarily negative. Hence, when it exists, the equilibrium point is always stable. ■

Based on these local stability results and on Lemma 2, we formulate the main result of this section that characterizes the asymptotic behavior of Eq. (4).

Theorem 1. *Consider the coupled system in Eq. (4) under Assumption 2. Then, for almost every initial condition $\mathbf{x}(0) = (I(0), P(0))$, the following four mutually exclusive and exhaustive scenarios can occur:*

- 1) if $\beta(0) < 1$, then the dynamics converges to the DFE $\mathbf{x}^{(1)}$;
- 2) if $1 < \beta(0) < (1 - \alpha^{-1}(0))^{-1}$, then the dynamics converges almost everywhere (a.e.) to the EE $\mathbf{x}^{(3)}$;
- 3) if $\beta(0) > (1 - \alpha^{-1}(0))^{-1}$ and $\beta(1) < (1 - \alpha^{-1}(0))^{-1}$, then the dynamics converges a.e. to the EE $\mathbf{x}^{(5)}$;
- 4) if $\beta(1) > (1 - \alpha^{-1}(0))^{-1}$, then the dynamics converges a.e. to the EE $\mathbf{x}^{(4)}$,

where the equilibria $\mathbf{x}^{(1)}$, $\mathbf{x}^{(3)}$, $\mathbf{x}^{(4)}$ and $\mathbf{x}^{(5)}$ are defined in Proposition 1.

Proof: To prove the convergence we use the Poincaré–Bendixson Theorem [46] and the result of Lemma 2, where we have ruled out the existence of periodic orbits in the region $[0, 1] \times [0, 1]$. We consider the four different cases in the statement:

- 1) If $\beta(0) < 1$, Lemma 1 guarantees that Eq. (4) has only two equilibria: $\mathbf{x}^{(1)}$, which is locally asymptotically stable, and $\mathbf{x}^{(2)}$, which is fully unstable. The Poincaré–Bendixson theorem ensures that the ω -limit set reduces to the unique locally stable equilibrium $\mathbf{x}^{(1)}$.
- 2) We split the case $1 < \beta(0) < (1 - \alpha^{-1}(0))^{-1}$ in two sub-cases:
 - a) If $\beta(1) < 1$, Lemma 1 concludes that Eq. (4) has three equilibrium points: the locally asymptotically stable $\mathbf{x}^{(3)}$, and two saddle points $\mathbf{x}^{(1)}$ and $\mathbf{x}^{(2)}$. The stable manifold of the two saddle points $\mathbf{x}^{(1)}$ and $\mathbf{x}^{(2)}$ is given by $I = 0$ and $P = 1$, respectively. Hence, for any initial condition in the region $(0, 1] \times [0, 1)$, the Poincaré–Bendixson Theorem guarantees global

asymptotic stability of $\mathbf{x}^{(3)}$. This yields global convergence for almost every initial condition.

- b) If $\beta(1) > 1$, Lemma 1 guarantees that Eq. (4) has four equilibria: the locally asymptotically stable $\mathbf{x}^{(3)}$, two saddle points $\mathbf{x}^{(1)}$ and $\mathbf{x}^{(4)}$ with stable manifolds $I = 0$ and $P = 1$, respectively, and the fully unstable equilibrium $\mathbf{x}^{(2)}$. The same argument used in the above applies also to this scenario, guaranteeing global convergence for almost every initial condition.
- 3) If $\beta(0) > (1 - \alpha^{-1}(0))^{-1}$ and $\beta(1) < (1 - \alpha^{-1}(0))^{-1}$, then from Lemma 1 we observe that $\mathbf{x}^{(5)}$ is the only locally asymptotically stable equilibrium point, while the others fixed points are either fully unstable equilibria or saddle points. Specifically, the stable manifolds of such saddle points are the regions $P = 0$, $P = 1$ and $I = 0$. Hence, using the Poincaré–Bendixson Theorem we guarantee convergence to $\mathbf{x}^{(5)}$ from any initial condition in $(0, 1] \times (0, 1)$, and thus for almost every initial condition in the domain.
- 4) If $\beta(1) > (1 - \alpha^{-1}(0))^{-1}$, then from Lemma 1 the system has four equilibria: $\mathbf{x}^{(4)}$, which is locally asymptotically stable, $\mathbf{x}^{(1)}$ and $\mathbf{x}^{(3)}$, which are saddle points, and $\mathbf{x}^{(2)}$, which is unstable. The stable manifolds of the saddle points are $P = 1$ and $I = 0$. Again, Poincaré–Bendixson Theorem yields convergence. ■

Remark 2. As a consequence of Theorem 1, the sole quantity $\beta(0)$ determines the epidemic threshold of the model. In fact, for $\beta(0) < 1$, the DFE is globally asymptotically stable; for $\beta(0) > 1$, the system converges a.e. to an EE. The functions α and β , instead, determines which EEs is reached above the epidemic threshold.

A. LINEAR CASE

We consider a specialization of our model to illustrate the findings presented in Theorem 1. Specifically, we focus on the case introduced in Example 1, where $\beta(P)$ and $\alpha(I)$ are linear functions, and the system reduces to Eq. (7). Focusing on the equilibria of the system and following the results of Sec. III, we obtain the following corollary, which provides an explicit expression for all the equilibria of the system.

Corollary 1. *The system in Eq. (7) has at most the following five equilibria:*

- 1) the DFE $\mathbf{x}^{(1)} = (0, 0)$, which is (locally) stable if $\beta_0 < 1$ and an (unstable) saddle point if $\beta_0 > 1$;
- 2) the DFE $\mathbf{x}^{(2)} = (0, 1)$, which is always unstable;
- 3) the EE $\mathbf{x}^{(3)} = (1 - \frac{1}{\beta_0}, 0)$, which exists iff $\beta_0 > 1$ and is stable iff $d > d^{(3)} = 1 - \frac{1}{\beta_0}$;
- 4) the EE $\mathbf{x}^{(4)} = (1 - \frac{1}{(1-a)\beta_0}, 1)$, which exists iff $\beta_0 > 1/(1-a)$ and it is stable iff $d < d^{(4)} = 1 - \frac{1}{(1-a)\beta_0}$;

- 5) the EE $\mathbf{x}^{(5)} = (d, \frac{\beta_0(d-1)-1}{a\beta_0(d-1)})$, which exists and is stable iff $\beta_0 > 1$ and either (a) $(1-a)\beta_0 \leq 1$ and $d < d^{(3)}$, or (b) $(1-a)\beta_0 \geq 1$ and $d^{(4)} < d < d^{(3)}$.

Then, we can apply Theorem 1, which guarantees that the dynamics converges a.e. to a stable equilibrium point. Specifically, we observe that the difficulty of adopting self-protective behavior d is a key parameter to determine which equilibrium is stable, together with the basic reproduction number β_0 and the efficacy of self-protective behavior a , as summarized in the following corollary. A graphic representation of the equilibria by varying d is depicted in Fig. 1.

Corollary 2. *The following four asymptotic behaviors are possible for the system in Eq. (7):*

- 1) If $\beta_0 < 1$, then the system converges to the DFE $\mathbf{x}^{(1)}$.
- 2) If $\beta_0 > 1$ and $d > d^{(3)}$ the system converges to the EE $\mathbf{x}^{(3)}$, i.e., the difficulty of the behavior prevents from its adoption.
- 3) If $\beta_0 > 1$ and $d < d^{(3)}$, then
 - a) if $(1-a)\beta_0 < 1$ or $(1-a)\beta_0 > 1$ and $d > d^{(4)}$, the system converges to the EE $\mathbf{x}^{(5)}$, in which part of the population adopts self-protective behavior;
 - b) if $(1-a)\beta_0 > 1$ and $d < d^{(4)}$, then the system converges to the EE $\mathbf{x}^{(4)}$ where the whole population adopts self-protective behavior.

Remark 3. From Corollary 2, we observe that d has a key role. In fact, when above the epidemic threshold $\beta_0 > 1$, decreasing the difficulty of adopting self-protective behavior allows to switch from the EE $\mathbf{x}^{(3)}$ to $\mathbf{x}^{(5)}$, in which there are less infected individuals. Moreover, if $a\beta_0 > 1$, a further decrease of d could lead to the EE $\mathbf{x}^{(4)}$, in which the fraction of infected individuals is further decreased.

IV. CONTROL

We study the problem of designing optimal policies to control our epidemic–behavioral model. In particular, we focus on the linear scenario in Example 1. We consider policies that promote safe practices by reducing the difficulty of adopting self-protective behavior, captured by the parameter d . These policies include increasing the availability of protection devices, reducing their costs, or raising awareness. To model such interventions, we modify the term α in Eq. (7) by splitting the term d into two contributions, i.e., $d = d_N - u$, where d_N is a baseline difficulty to adopting self-protective behavior in the absence of any interventions, and u captures instead the effect of containment regulations and should be interpreted as a control parameter. Hence, we obtain

$$\alpha(I) = I - (d_N - u). \quad (11)$$

We observe that the control parameter u can theoretically take both positive and negative values (greater than $-d_N$), which corresponds to incentives or disincentives to engage in

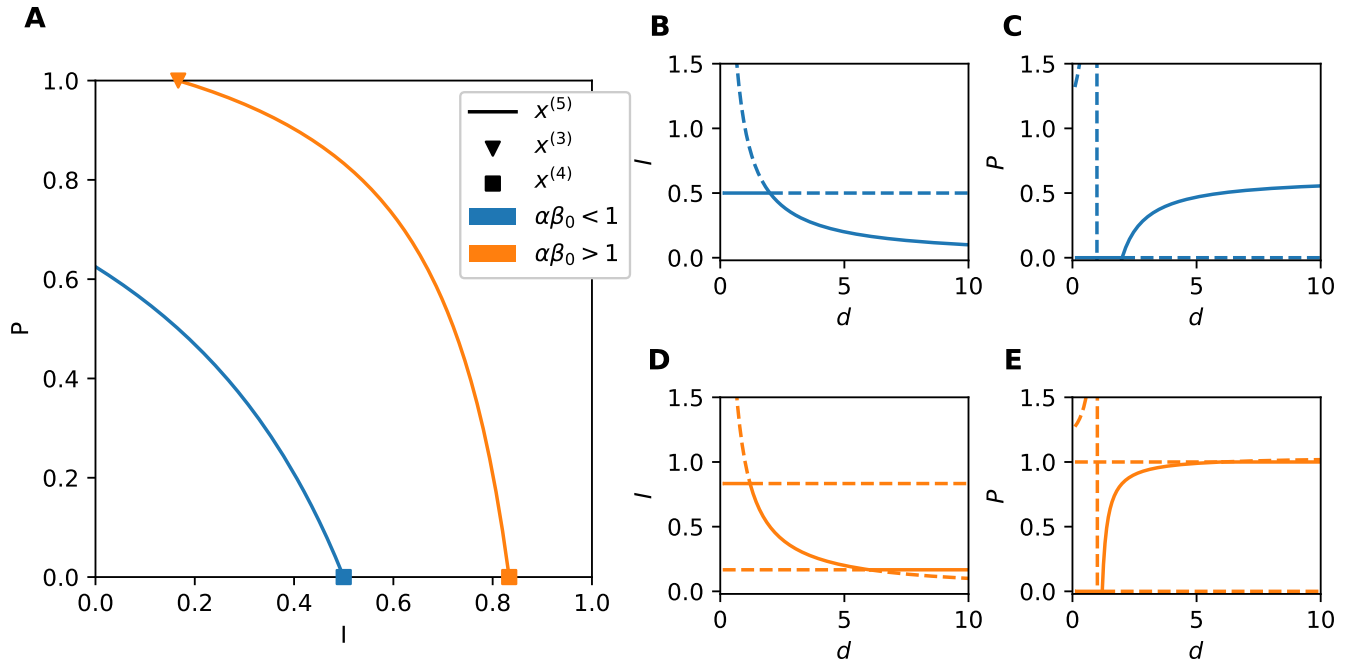


FIGURE 1. Equilibria in the linear case. In (A), we illustrate the equilibria in the space (I, P) by varying d for $\beta_0 > 1$ and $\alpha\beta_0 < 1$ (blue) or $\alpha\beta_0 > 1$ (orange). Steady state value of I and P for different values of d for $\alpha\beta_0 < 1$ are reported in (B,C), respectively; and for $\alpha\beta_0 > 1$ in (D,E), respectively.

self-protective behavior. Hence, the controlled system under investigation ultimately reads as

$$\begin{cases} \dot{I} = \beta_0((1-P) + (1-a)P)(1-I)I - I \\ \dot{P} = \tilde{\varepsilon}(I - d_N + u)P(1-P). \end{cases} \quad (12)$$

From Theorem 1, we observe that the control input u does not affect the stability of the DFE, which is fully determined by the infection rate β . However, as we shall see, it yields a change in the EE to which the system converges to, when above the epidemic threshold. Hence, a proper choice of u may lead to effective containment policies to contrast the spreading of the epidemic. For this reason, in the rest of this paper we will focus on scenarios in which $\beta_0 > 1$, and the system converges to an EE. Since the stable EE is unique and fully determined by the model parameters, in our setting it will be function of the control input, and we will refer to it as $\mathbf{x}^*(u) = (I(u), P(u))$, for which an explicit expression can be found using Corollaries 1 and 2.

In order to formalize the optimal control problem, we start by defining a cost function. The purpose of epidemic management is to design interventions to reduce the number of infected individuals while balancing the social and economical impact of the interventions implemented. In particular, to a control input u , we associate a cost function that accounts for these two critical factors by taking a convex combination of two quadratic terms: one in the number of infected individuals, the other in the effort placed in interventions. Hence, we obtain the following cost function:

$$J_h(u) = hI(u)^2 + (1-h)u^2, \quad (13)$$

where the two summands are weighted by the parameter $h \in [0, 1]$, which captures the relative weight given to reducing the healthcare impact with respect to the economic cost associated with the implementation of the interventions. The use of quadratic terms in Eq. (13) is the simplest and most common choice in mathematical epidemiology [47], since it captures the nonlinear increase of the burden for the healthcare system associated with the number of infections [48], and the fact that interventions are often characterized by diminishing marginal returns [49].

A. STATIC INTERVENTION POLICIES

We start by investigating optimal static intervention policies. Given a certain cost function $J_h(u)$ (defined by the trade-off parameter h), our aim is to determine the optimal intervention strategy u^* and the associated steady state that minimize this cost \mathbf{x}^* . Intuitively, placing more emphasis on the healthcare impact by increasing h would result in an increase in the control effort u^* and less infections at the steady state. However, as demonstrated below, due to threshold effects, the impact of these interventions may not always yield the desired outcome.

We evaluate J_h at the EE, which we know to be either $\mathbf{x}^{(3)}$, $\mathbf{x}^{(4)}$, or $\mathbf{x}^{(5)}$ (see Corollary 2). Evaluating the cost function at such stable equilibrium by varying u result in a piecewise continuous function composed by three pieces:

$$J_h(u) = \begin{cases} h \left(\frac{\beta_0 - 1}{\beta_0} \right)^2 + (1-h)u^2 & \text{if } u < d_N - d^{(3)}, \\ h \left(\frac{(1-a)\beta_0 - 1}{(1-a)\beta_0} \right)^2 + (1-h)u^2 & \text{if } u > d_N - d^{(4)}, \\ u^2 - 2hd_Nu + hd_N^2 & \text{otherwise.} \end{cases} \quad (14)$$

In the case of static intervention policies, our goal is to identify the optimal control input that minimizes the cost function in Eq. (13), i.e., $u^* := \operatorname{argmin}_u J_h(u)$. To analytically solve this problem, we compare the local minima of the cost function in each of the three pieces. This comparison results in different scenarios depending on the system equilibrium without interventions (i.e., $u = 0$), as summarized in the following result.

Theorem 2. *The optimal control policy for Eq. (12) with the cost function in Eq. (13) is attained with control input equal to*

$$u^* = \begin{cases} d_N h & \text{if } \Omega_1 \text{ holds,} \\ d_N - d^{(4)} & \text{if } \Omega_2 \text{ holds,} \\ 0 & \text{otherwise,} \end{cases} \quad (15)$$

where $\Omega_1 := \left\{ d^{(3)} < d_N < \frac{(d^{(3)})^2}{d^{(4)}} \text{ and } 1 - \left(\frac{d^{(3)}}{d_N}\right)^2 \leq h \leq 1 - \frac{d^{(4)}}{d_N}; \text{ or } d^{(4)} \leq d_N \leq d^{(3)} \text{ and } h \leq 1 - \frac{d^{(4)}}{d_N} \right\}$ and $\Omega_2 := \left\{ d^{(3)} < d_N < \frac{(d^{(3)})^2}{d^{(4)}} \text{ and } h > 1 - \frac{d^{(4)}}{d_N}; \text{ or } d_N > \frac{(d^{(3)})^2}{d^{(4)}} \text{ and } h \geq \frac{(d_N - d^{(4)})^2}{(d^{(3)})^2 + d_N^2 - 2d_N d^{(4)}}; \text{ or } d^{(4)} \leq d_N \leq d^{(3)} \text{ and } h > 1 - \frac{d^{(4)}}{d_N} \right\}$, yielding the controlled epidemic-behavioral system in Eq. (7) to converge to the EE:

$$\mathbf{x}^* = \begin{cases} \mathbf{x}^{(3)} & \text{if } d_N > d^{(3)} \text{ and } h \leq 1 - \left(\frac{d^{(3)}}{d_N}\right)^2, \\ \tilde{\mathbf{x}} & \text{if } d^{(3)} < d_N < \frac{(d^{(3)})^2}{d^{(4)}} \\ & \text{and } 1 - \left(\frac{d^{(3)}}{d_N}\right)^2 \leq h \leq 1 - \frac{d^{(4)}}{d_N}, \\ & \text{or } d^{(4)} \leq d_N \leq d^{(3)} \text{ and } h \leq 1 - \frac{d^{(4)}}{d_N}, \\ \mathbf{x}^{(4)} & \text{otherwise,} \end{cases} \quad (16)$$

where $\mathbf{x}^{(3)}$ and $\mathbf{x}^{(4)}$ are defined in Corollary 1 and

$$\tilde{\mathbf{x}} = \left((1-h)d_N, \frac{\beta_0 - 1 - \beta_0(1-h)d_N}{\beta_0((1-h)d_N - 1)(a-1)} \right). \quad (17)$$

Proof: First, we observe some properties of the cost function in Eq. (13). In the first and last open intervals, the cost is a quadratic function in u , thus increasing in the absolute value of u . In addition we observe that these two open intervals correspond to the conditions for stability of $\mathbf{x}^{(3)}$ and $\mathbf{x}^{(4)}$, respectively. In the compact interval $u \in [d_N - d^{(3)}, d_N - d^{(4)}]$, the cost is instead a convex function, and this interval corresponds to the conditions for stability of $\mathbf{x}^{(5)}$.

We focus now on the local minima of the cost function. Since the function is convex in $u \in [d_N - d^{(3)}, d_N - d^{(4)}]$, then it has a unique local minimum in that compact set. This minimum is either at $\hat{u} = d_N h$, if $\hat{u} \in [d_N - d^{(3)}, d_N - d^{(4)}]$, or at one of its boundaries. Whether the function has other local minima in the two unbounded intervals depends on the interval to which $u = 0$ belongs. If $0 \in [d_N - d^{(3)}, d_N - d^{(4)}]$, i.e., $d_N \in [d^{(4)}, d^{(3)}]$, then the function is monotonically increasing with $|u|$ in both regions, yielding that the infimum is attained in the limits $u \rightarrow d_N - d^{(3)}$ and $u \rightarrow d_N - d^{(4)}$. Continuity of the function guarantees that the function has its unique local minimum in the compact set $[d_N - d^{(3)}, d_N - d^{(4)}]$, which is thus global (see Fig. 2A).

In the following, we will thus consider three scenarios depending on the interval $u = 0$ belongs to. If $d_N > d^{(3)}$, then the function has a local minimum at $u = 0$, which is in the first region of the piecewise function in Eq. (13) (see Figs. 2B–C). Then, we observe that in the compact interval $[d_N - d^{(3)}, d_N - d^{(4)}]$, the candidate local minimum $\hat{u} = d_N h$ belongs to the interval iff

$$d_N - d^{(3)} \leq h d_N \leq d_N - d^{(4)} \iff 1 - \frac{d^{(3)}}{d_N} \leq h \leq 1 - \frac{d^{(4)}}{d_N}. \quad (18)$$

Being $d^{(4)} < d^{(3)} < d_N$, the region in Eq. (18) is always well defined. If $h < 1 - \frac{d^{(3)}}{d_N}$, then the local minimum is attained at the boundary point $\tilde{u}_1 = d_N - d^{(3)}$; if $h > 1 - \frac{d^{(4)}}{d_N}$, the local minimum is attained at the boundary point $\tilde{u}_2 = d_N - d^{(4)}$.

The global minimum is determined by comparing the cost at $u = 0$, which is equal to $J_h(0) = h(d^{(3)})^2$ with the cost at the other local minimum. For $h < 1 - \frac{d^{(3)}}{d_N}$, it is straightforward to observe that, due to the continuity of the cost function, $J_h(0) < J_h(\tilde{u}_1)$. For $1 - \frac{d^{(3)}}{d_N} \leq h \leq 1 - \frac{d^{(4)}}{d_N}$, we obtain $J_h(\hat{u}) = h(1-h)d_N^2$, obtaining the condition

$$J_h(\hat{u}) \leq J_h(0) \iff h \geq 1 - \left(\frac{d^{(3)}}{d_N}\right)^2, \quad (19)$$

which yields a nonempty set when coupled with $h \leq 1 - \frac{d^{(4)}}{d_N}$ iff $d_N < \frac{(d^{(3)})^2}{d^{(4)}}$. If $h > 1 - \frac{d^{(4)}}{d_N}$, the other local minimum is $\tilde{u}_2 = d_N - d^{(4)}$, and the associated cost is equal to $J_h(\tilde{u}_2) = h(d^{(4)})^2 + (1-h)(d_N - d^{(4)})^2$, obtaining the condition

$$J_h(\tilde{u}) \leq J_h(0) \iff h \geq \frac{(d_N - d^{(4)})^2}{(d^{(3)})^2 + d_N^2 - 2d_N d^{(4)}}. \quad (20)$$

We observe that such a condition is more restrictive than $h > 1 - \frac{d^{(4)}}{d_N}$ iff $d_N > \frac{d^{(3)}}{d^{(4)}}$.

If $d_N \in [d^{(4)}, d^{(3)}]$, then the global minimum is the unique minimum in the compact interval $[d_N - d^{(3)}, d_N - d^{(4)}]$, which is u^* if such a candidate belongs to the interval, i.e., if $h d_N < d_N - d^{(4)} \implies h < 1 - d^{(4)}/d_N$, and is equal to $\tilde{u} = d_N - d^{(4)}$, otherwise.

If $d_N < d^{(4)}$, then the function has another local minimum at $u = 0$, which is in the third region of Eq. (13). In this scenario, the global minimum is determined by comparing the cost at $u = 0$, which is equal to $J_h(0) = h\left(\frac{(1-a)\beta_0 - 1}{(1-a)\beta_0}\right)^2$, and the cost at the local minimum in the compact set, which is always attained at $\tilde{u} = d_N - d^{(4)}$. From the comparison, it is straightforward that $J_h(0) < J_h(\tilde{u})$.

Finally, we complete the proof by computing, for each control, the corresponding EE, obtaining Eq. (16). ■

Theorem 2 provides an insightful characterization of the optimal control input, depending on the model parameters and on the cost trade-off h , as discussed in the following.

Remark 4. *The baseline difficulty of adopting self-protective behavior d_N has a key role. In fact, if d_N is larger than $d^{(3)}$, the population would not adopt self-protection in the absence of any control, yielding the EE $\mathbf{x}^{(3)}$. In the controlled*

system, the trade-off parameter h yields a threshold behavior. Namely, if h is small, the optimal solution would be to not apply any control, remaining in $\mathbf{x}^{(3)}$; if h is sufficiently large, the optimal control is not null and reaches an EE with less infected individuals with respect to the uncontrolled case. The value of the threshold is a function of the model parameters. As d_N decreases, an intermediate regime is reached, where in the application of a nonzero control input to decrease the number of infections is always optimal. Finally, unsurprisingly, if d_N is even smaller, then the entire population would adopt self-protection even in the absence of any control, making the control input unnecessary.

To conclude, in the first scenario described of self-protections difficult to adopt (large d_N), it is worth noticing from Fig. 2B that starting from $u = 0$ there is an initial increase in the cost, due to nonconvexity of the cost function, discouraging intervention implementation, before notice the advantage of the interventions, highlighting the nontriviality of the results in Theorem 2.

B. DYNAMIC INTERVENTION POLICIES

In the previous section, we have analyzed the problem of determining an optimal control input to trade-off the healthcare impact and economic cost of an endemic disease in a steady-state scenario. We now focus on a different problem, i.e., to determine the optimal, possibly varying, intervention policy $u(t)$ in a dynamically-evolving environment, i.e., when the system is in a transient phase.

Specifically, in the previous section we showed how, given the cost function $J_h(u)$ in Eq. (13), we can calculate the optimal (static) intervention policy \hat{u} and the corresponding steady state \mathbf{x}^* . Here, we consider a system with initial conditions at $t = t_0$ that are not optimal with respect to such cost function, namely $\mathbf{x}_0 \neq \mathbf{x}^*$. Our goal is to steer the system to the desired optimal final steady state \mathbf{x}^* within a time-horizon of duration T , while minimizing the cost function along the entire system trajectory. To this aim, we naturally extend the definition of the cost function in Eq. (13) to a dynamically-evolving setting, with quadratic cost at time t equal to $J_h(\mathbf{x}(t), u(t)) = hI^2(t) + (1-h)u^2(t)$, where $\mathbf{x}(t) = (I(t), P(t))$ is the state of the epidemic-behavioral system at time t , which evolves according to the following nonautonomous, nonlinear system:

$$\begin{cases} \dot{I} = \beta_0((1-P) + (1-a)P)(1-I)I - I \\ \dot{P} = \tilde{\varepsilon}(I - d_N + u(t))P(1-P). \end{cases} \quad (21)$$

We can now define an optimal control problem, which takes the form of the nonlinear quadratic regulator

$$\begin{aligned} & \min_{u(t)} \int_{t_0}^T J_h(\mathbf{x}(t), u(t))dt + \phi(\mathbf{x}(T)), \\ & \text{subject to} \quad \text{Eq. (21)} \\ & \quad \mathbf{x}(t_0) = \mathbf{x}_0, \\ & \quad u_l \leq u(t) \leq u_u. \end{aligned} \quad (22)$$

Notably, we seek for a control function $u(t)$, bounded between a lower and an upper bound $[u_l, u_u] \subseteq \mathbb{R}$, which minimizes the integrated cost function along the entire trajectory plus an terminal cost $\phi(\mathbf{x}(T))$ computed at the final time T . Since our primary goal is to control the transient behavior of the system while steering it toward the desired state \mathbf{x}^* at the time T , we use a terminal cost to penalize control inputs that result in the system being far from the desired state at the final time, i.e.,

$$\phi(\mathbf{x}(T)) = \varphi \|\mathbf{x}(T) - \mathbf{x}^*\|_2. \quad (23)$$

The parameter $\varphi \geq 0$ is a constant that weights the contribution of the terminal cost and should be set to obtain a trajectory that ends close enough to \mathbf{x}^* [50]. We observe that we do not enforce a hard constraint on the final system state. Therefore, the optimal control policy does not guarantee that the system reaches the equilibrium point precisely at time T , but it guarantees that the system approaches its target by penalizing deviations, avoiding issues related to infeasibility. Then, if one wants to enforce convergence to the desired target state, one can leverage Corollary 1 and (if feasible) set $u(t) = d_N - I^*$ for all $t \geq T$, ensuring convergence of the epidemic prevalence to I^* by Corollary 2.

The control problem in Eq. (22) can be solved using the Pontryagin's Maximum Principle (PMP) [41], whose result is summarized in the following proposition.

Proposition 2. *The optimal control for the problem in Eq. (22) satisfies the following necessary condition:*

$$u(t) = \min \left\{ u_l, \max \left\{ u_u, -\frac{\lambda_2(t)(P(t)-1)P(t)\varepsilon}{2(h-1)} \right\} \right\}, \quad (24)$$

where $\boldsymbol{\lambda}(t) := [\lambda_1(t), \lambda_2(t)]^\top$ is the two co-state variable that evolves according to

$$\dot{\boldsymbol{\lambda}} = -\nabla_{\mathbf{x}}(H(t, \mathbf{x}, u, \boldsymbol{\lambda})), \quad (25)$$

with

$$H(t, \mathbf{x}, u, \boldsymbol{\lambda}) = J_h(\mathbf{x}(t), u(t)) + \lambda_1(t)\dot{I}(t) + \lambda_2(t)\dot{P}(t). \quad (26)$$

Proof: According to PMP, the necessary condition for a control $u(t)$ to be optimal is that the Hamiltonian function in Eq. (26) attains its minimum value. The co-state variables vector $\boldsymbol{\lambda}(t)$ evolves alongside the state variable defining a two-point boundary value problem that couples Eq. (21) and Eq. (25), with boundary conditions $\mathbf{x}(t_0) = \mathbf{x}_0$ and $\boldsymbol{\lambda}(T) = \nabla_{\mathbf{x}(T)}\phi(\mathbf{x}_T)$. The optimal control $u(t)$ can be obtained by solving $u(t) = \arg \min_u H(t, \mathbf{x}, u, \boldsymbol{\lambda})$, which is equivalent to solve the equation $\frac{\partial H(t, \mathbf{x}, u, \boldsymbol{\lambda})}{\partial u} = 0$, which inserted in the Hamiltonian in Eq. (26), yields $u^*(t) = -\frac{\lambda_2(t)(P(t)-1)P(t)\varepsilon}{2(h-1)}$. Since the control is bounded, the unconstrained minimizer of the Hamiltonian $u^*(t)$ may fall out of the constant $u(t) \in [u_l, u_u]$. Following the derivation in [42], we saturate it to the value of the lower and upper bound, finally obtaining the expression in Eq. (24). ■

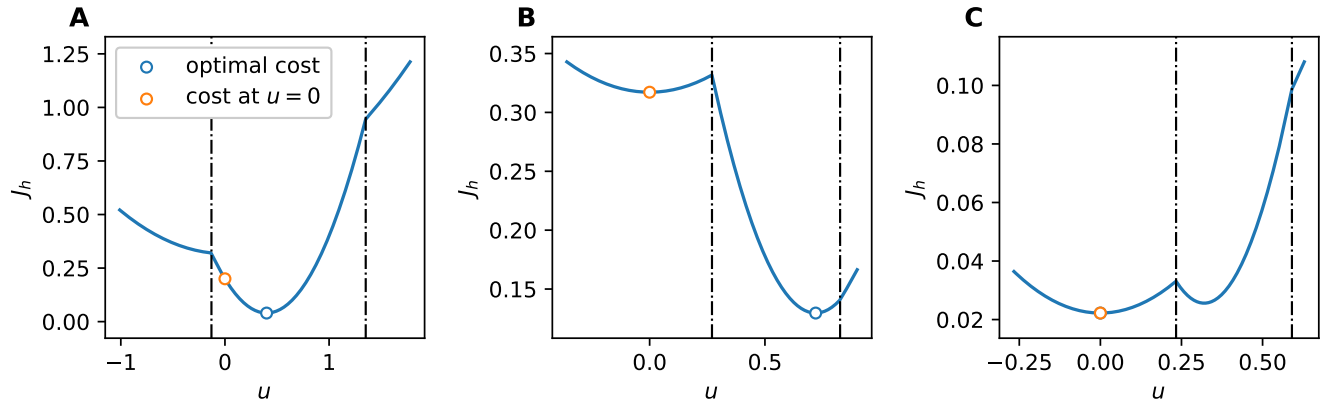


FIGURE 2. Examples of cost functions. In (A), the steady state $x^{(5)}$ is stable without interventions. In (B) and (C), in the absence of control, the equilibrium point is $x^{(3)}$. In (B), the optimal cost is located in the convex part of the function, while, in (C), it is $\hat{u} = 0$.

From a practical point of view, the two-point boundary value problem that couples Eq. (21) and Eq. (25), is solved numerically over the time horizon $[t_0, T]$ and the solution is inserted into Eq. (24). The time-horizon T may be imposed by public authorities, or obtained by solving an optimization problem, which can be either independent, or solved jointly with the optimal control problem. For more details, see [42].

While our approach employs established techniques from optimal control theory, interesting insights are gained in the next section when applying this framework to a case study.

V. CASE STUDY: APPLICATION TO STI

We demonstrate our approach by applying it to a case study based on STIs—a class of diseases that are endemic in the population, whose spread is significantly influenced by human behavior. Despite the fact that STIs are typically not fatal, they constitute a serious threat to healthcare and the economy worldwide. Remarkably, the WHO estimated 374 million people got infected with an STI in 2020, and the 19.7 million cases in 2008 in the US had an estimated direct medical cost of roughly \$15.6 billion. These figures highlight the importance of the design of an optimal control strategy to incentivize the adoption of self-protective behavior.

A. EPIDEMIC PARAMETERS

We calibrate our model to gonorrhea, for which condoms are the most widely used equipment for self protection, with an estimated average efficacy of $a = 0.87$, considering also usage errors [51]. From a survey study conducted in 1999 in the US, condoms were used in 62% of occurrences between casual partners [52]. Lower fractions were reported in a more recent study (37%) [53]. Here, we set an intermediate values of $P_0 = 0.5$. In an epidemiological study carried out in the US in 2018, it was estimated that the prevalence of gonorrhea infections is of 190 infections per 100,000 population [54]. Based on this data, we set the initial fraction of infections at $I_0 = 0.0019$. From these parameters, assuming that the disease is at steady state, we use the explicit expression of $x^{(5)}$ in Corollary 1 to derive $d = 0.019$ and $\beta_0 = 1.77$.

Note that our estimation of the basic reproduction number is consistent with estimations based on clinical data, available in the literature [55].

As the data we use for this calibration refer to a system in which some intervention policies (e.g., awareness campaigns) are already implemented, to reduce our setting to the one in Sec. A we split d in the sum of a baseline value d_N and initial control input $u(0)$. To this aim, we assume that in absence of control policies ($u = 0$) the cost of using protection and the risk perceived by individuals is such that only a negligible fraction of the population would adopt self-protective behavior, i.e., we assume that $d_N = d^{(3)}$ and the system steady state in the absence of control settles at $x^{(3)}$. This further assumption yields $d_N = \frac{\beta_0 - 1}{\beta_0} = 0.436074$ and $u(0) = d - d_N = 0.434174$.

B. OPTIMAL INTERVENTIONS

We consider the scenario in which public health authorities need to reevaluate their interventions reflecting, e.g., a change in the price associated with protection devices, or in the healthcare, social, and economical cost associated with infected individuals. Formally, at $t = 0$, we consider the system in its current steady state x_0^* , with respect to a given cost function J_{h_0} . Then, we introduce a new cost function J_{h_1} , with its associated steady state x_1^* . The goal is to find the optimal intervention $u(t)$ to transition to the new optimal steady state x_1^* . We notice that x_1^* and x_0^* are related to the optimal steady interventions u_1^* and u_0^* , respectively, which define the initial and final values for the control variable. The case $h_1 > h_0$ represents an increase of the relative cost of infected individuals with the consequent increase in the containment policies to reduce the number of infected. On the other hand, $h_1 < h_0$ reflects uplifting some containment measures. We use as x_0^* , h_0 , and u_0^* the values of the calibrated model obtained in Sec. V. We test six scenarios where x_1^* has $\pm 10\%$, $\pm 20\%$, and $\pm 50\%$ fraction of infected individuals. The value of u_l and u_u are such that $u(t)$ can exceed the initial and final control u_0 and u_1 by 50% of the total variation $|u_0^* - u_1^*|$. Following [42], the time-

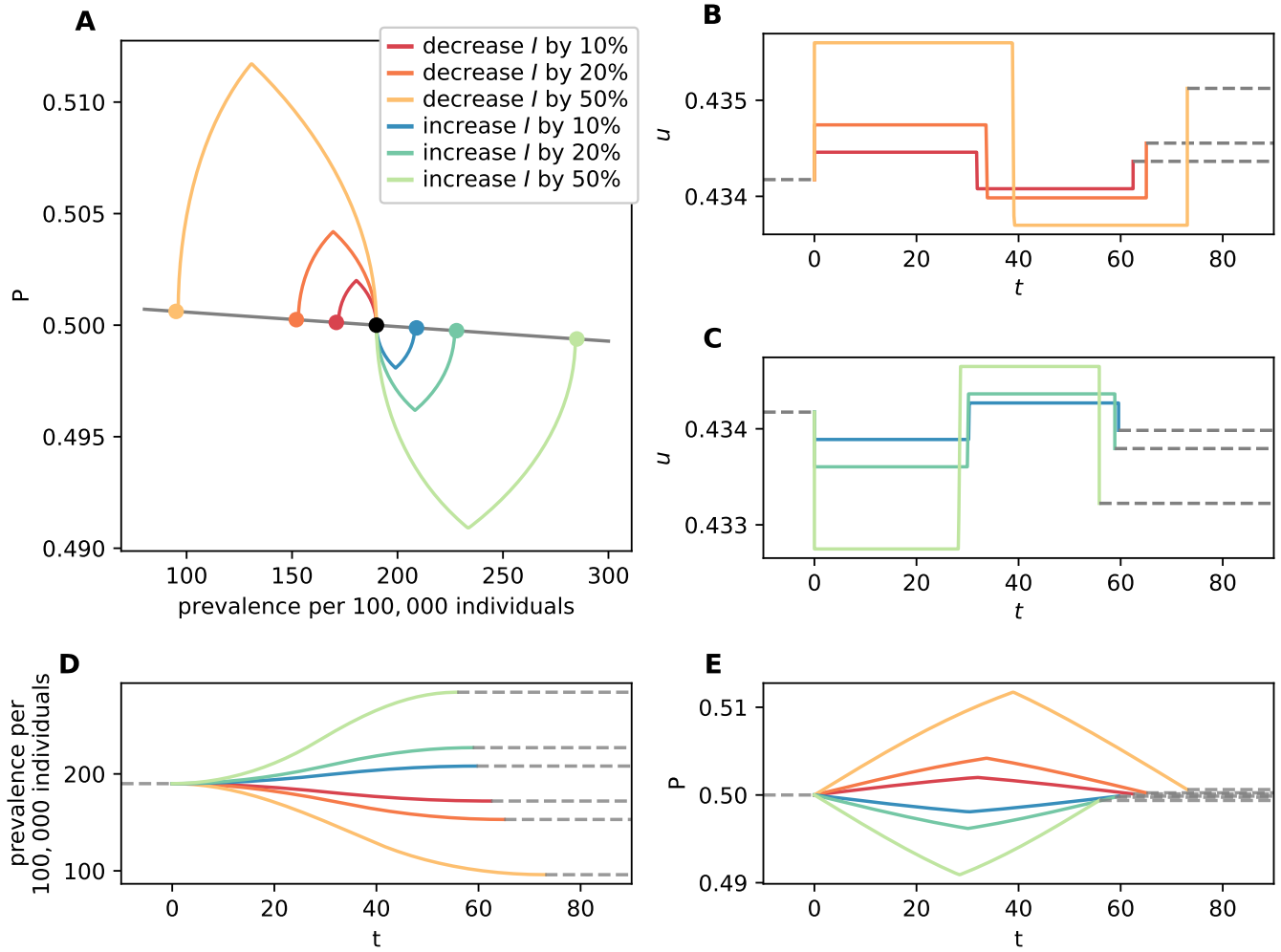


FIGURE 3. Simulation results of the STIs case study. In (A), the optimal trajectory for different desired end points x_1^* are illustrated; the black dot is the starting point of the system x_0^* . In (B, C), the optimal control inputs for the corresponding scenarios in panel (A) are reported. In (D,E), the temporal evolutions of the state variables $I(t)$ and $P(t)$ are reported, respectively.

horizon T is selected as the minimum time that allows the controlled system to reach the desired final state x_1^* with a certain tolerance (set to 10^{-5}), and is computed numerically by solving the problem for increasing values of T , until one that satisfies the constraint is obtained.

The optimal policies $u(t)$ are found using Proposition 2 and plotted in Fig. 3. Our simulations suggest that the optimal interventions are piecewise constant. An initial period entails implementing strong interventions in case $u_1^* > u_0^*$, or relaxing them if $u_1^* < u_0^*$. Then, the opposite action is taken and, finally, at $t = T$, it is set $u(T) = u_1^*$, so that the desired ending point becomes an equilibrium. From a practical point of view, the devised optimal strategy is straightforward to implement, as only two actions with constant effort must be implemented. Proposition 2 is key to understand the right time of switching between the two actions. From Fig. 3, we observe that the timing and trajectories are not symmetric between increasing or decreasing the policy of intervention.

Finally, we explore the effect of the parameter $\tilde{\varepsilon}$ using the case study from the previous example, which involves a 50% reduction in disease prevalence. The parameter $\tilde{\varepsilon}$ measures the population's reactivity in changing behavior and is defined as $\tilde{\varepsilon} = w\varepsilon$, where ε represents the rate at which the revision process occurs (see Eq. (3)), and w is a proportional coefficient capturing the reactivity of the population's behavioral response (see Eq. (6)). Small values of $\tilde{\varepsilon}$ characterize a population that changes the behavior slowly in response to the spreading of the disease, while large values indicate fast-reacting populations. In Fig. 4, we compute the optimal control policy for different values of $\tilde{\varepsilon}$. In all cases, the number of infected individuals remains between the initial and final states during the whole transient, and the optimal strategy is a two-action piecewise constant strategy as previously discussed. However, we observe that, for larger values of $\tilde{\varepsilon}$, the system is faster in reaching the desired final state, but larger oscillations in the transient are observed.

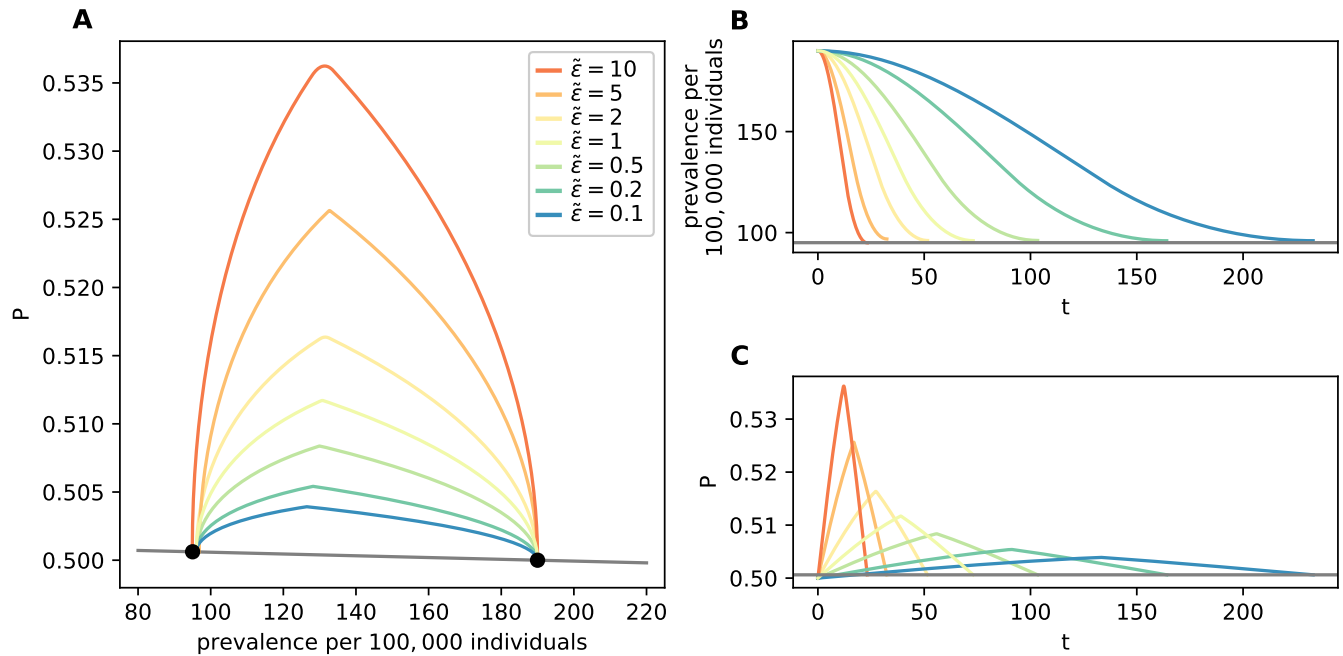


FIGURE 4. Simulation results of the STIs case study, exploring the impact of parameter ε . In (A), we illustrate the optimal trajectory for different values of ε . In (B, C), we report the temporal evolution of the state variables $I(t)$ and $P(t)$ for different values of ε , respectively.

VI. CONCLUSION

We presented an epidemic-behavioral model aimed at devising optimal intervention strategies that encourage the adoption of self-protecting behaviors. Our model takes into account both healthcare and socio-economic factors to ensure comprehensive control measures. Specifically, we employed an SIS-like epidemic dynamics and a population game dynamics, and we coupled them in a feedback scheme that captures i) the impact of the epidemic spreading on the risk perception that pushes people to adopt self-protective behavior, and ii) the impact of human behavior on the infection rate. We formalized our model as a planar nonlinear system of ODEs, which can match a variety of scenarios by conveniently selecting the shape of the two feedback functions. Under reasonable assumptions, we performed a theoretical analysis of the model, characterizing all its five steady states and proving global convergence to one equilibrium, which depends on the model parameters. Interestingly, the system exhibits a double-threshold behavior. Whether the system converges to the DFE is determined by an epidemic threshold that is independent of human behavior. However, above such a threshold, a second threshold determines the EE reached, depending on the difficulty of adopting self-protective behavior. This phenomenon relates to many typical epidemiological phenomena, where the onset of the epidemic depends on intrinsic epidemiological parameters, and the spontaneous adoption of self-protective behavior cannot fully eradicate the disease, but it can mitigate it.

Further, we used the model to investigate the control of epidemic diseases. Specifically, we focused on the scenario where the feedback functions are linear, which is amenable to

thorough analytical treatment. After having introduced a control input, we formalized the problem of designing optimal interventions by defining an objective function that trades-off the healthcare and social-economical costs. The study of the objective function at the equilibrium provided insight into the characterization of the steady-state optimal control input, while the Pontryagin maximum principle was used to design optimal control strategies. Through the analysis of a real-world case study inspired by STIs, we observed that the optimal solutions are piecewise constant, suggesting that our tool can be used to determine the optimal switching time between different policies. The optimality of piecewise control inputs is consistent with what has been observed in the literature on optimal interventions in epidemic processes, e.g., in SIS and SIR models with isolation of infected or health/vaccination campaigns [56]–[58].

Our work is not exempt from limitations. First, we proposed our framework in the scenario of a homogeneous fully-mixed population. Extending this work to heterogeneous and structured scenarios is a key extension. In particular, considering meta-population structures is relevant for the study of sub-population at high risk of infection, called *core population* in the STI literature [59]. Technically, such extension can be performed by embedding the model onto a network, for which, e.g., monotonicity properties may be used [60]. Second, we built our framework using epidemic and behavioral models. The epidemic model can be readily tailored to more complex progression dynamics by simply adding some equations to the system, which are not directly in feedback with the behavioral dynamics (see, e.g., the models used for COVID-19 [15], [61] or Ebola [62]). Third,

the main results related to epidemic control are limited to cases where the basic reproduction number and the perceived advantage of self-protective behavior are linear functions of the state variables. Extending our theoretical results to nonlinear scenarios is nontrivial, as the proofs of Theorem 2 and Proposition 2 rely on the explicit form of these functions. Addressing this challenge is a key objective for future research. Finally, the approach and results proposed in this paper can serve as a foundation for improved models that incorporate more complex behavioral dynamics, such as delays in behavioral response, biased risk perceptions, and imperfect information on epidemic prevalence. Additionally, more realistic settings can be explored by integrating online data into the control algorithm. These enhancements may enable our paradigm to provide optimal control solutions for real-world epidemic outbreaks, thereby supporting public health authorities in planning effective interventions.

REFERENCES

- [1] R. Pastor-Satorras, C. Castellano, P. Van Mieghem, and A. Vespignani, "Epidemic processes in complex networks," *Rev. Mod. Phys.*, vol. 87, pp. 925–979, Aug 2015.
- [2] C. Nowzari, V. M. Preciado, and G. J. Pappas, "Analysis and control of epidemics: A survey of spreading processes on complex networks," *IEEE Control Syst. Mag.*, vol. 36, no. 1, pp. 26–46, 2016.
- [3] W. Mei, S. Mohagheghi, S. Zampieri, and F. Bullo, "On the dynamics of deterministic epidemic propagation over networks," *Annu. Rev. Control*, vol. 44, pp. 116–128, 2017.
- [4] P. E. Paré, C. L. Beck, and T. Başar, "Modeling, estimation, and analysis of epidemics over networks: An overview," *Annu. Rev. Control*, vol. 50, pp. 345–360, 2020.
- [5] L. Zino and M. Cao, "Analysis, prediction, and control of epidemics: A survey from scalar to dynamic network models," *IEEE Circ. Syst. Mag.*, vol. 21, no. 4, pp. 4–23, 2021.
- [6] K. Drakopoulos, A. Ozdaglar, and J. N. Tsitsiklis, "An efficient curing policy for epidemics on graphs," *IEEE Trans. Netw. Sci.*, vol. 1, no. 2, pp. 67–75, 2014.
- [7] V. M. Preciado, M. Zargham, C. Enyioha, A. Jadbabaie, and G. Pappas, "Optimal vaccine allocation to control epidemic outbreaks in arbitrary networks," in *52nd IEEE Conf. Decis. Control*, 2013, pp. 7486–7491.
- [8] S. Gracy, P. E. Paré, H. Sandberg, and K. H. Johansson, "Analysis and distributed control of periodic epidemic processes," *IEEE Trans. Control Netw. Syst.*, vol. 8, no. 1, pp. 123–134, 2021.
- [9] F. Della Rossa *et al.*, "A network model of Italy shows that intermittent regional strategies can alleviate the COVID-19 epidemic," *Nat. Comm.*, vol. 11, no. 1, p. 5106, 2020.
- [10] L. Zino, A. Rizzo, and M. Porfiri, "On assessing control actions for epidemic models on temporal networks," *IEEE Control Syst. Lett.*, vol. 4, no. 4, pp. 797–802, 2020.
- [11] Y. Yi, L. Shan, P. E. Paré, and K. H. Johansson, "Edge deletion algorithms for minimizing spread in SIR epidemic models," *SIAM J. Control Optim.*, vol. 60, no. 2, pp. S246–S273, Mar. 2022.
- [12] R. M. Kovacevic, N. I. Stilianakis, and V. M. Veliov, "A distributed optimal control model applied to COVID-19 pandemic," *SIAM J. Control Optim.*, vol. 60, no. 2, pp. S221–S245, Mar. 2022.
- [13] F. Blanchini, P. Bolzern, P. Colaneri, G. De Nicolao, and G. Giordano, "Optimal control of compartmental models: The exact solution," *Automatica*, vol. 147, p. 110680, 2023.
- [14] F. Parino, L. Zino, M. Porfiri, and A. Rizzo, "Modelling and predicting the effect of social distancing and travel restrictions on COVID-19 spreading," *J. R. Soc. Interface*, vol. 18, no. 175, p. 20200875, 2021.
- [15] F. Parino, L. Zino, G. C. Calafiore, and A. Rizzo, "A model predictive control approach to optimally devise a two-dose vaccination rollout: A case study on COVID-19 in Italy," *Int. J. Robust Nonlinear Control*, vol. 33, no. 9, pp. 4808–4823, 2023.
- [16] G. Calafiore, F. Parino, L. Zino, and A. Rizzo, "Dynamic planning of a two-dose vaccination campaign with uncertain supplies," *European J. Oper. Res.*, 2022.
- [17] D. H. Morris, F. W. Rossine, J. B. Plotkin, and S. A. Levin, "Optimal, near-optimal, and robust epidemic control," *Commun. Phys.*, vol. 4, no. 1, Apr. 2021.
- [18] J. J. Van Bavel *et al.*, "Using social and behavioural science to support COVID-19 pandemic response," *Nat. Hum. Behav.*, vol. 4, no. 5, pp. 460–471, 2020.
- [19] J. Bedson *et al.*, "A review and agenda for integrated disease models including social and behavioural factors," *Nat. Hum. Behav.*, vol. 5, no. 7, pp. 834–846, 2021.
- [20] S. Funk, M. Salathé, and V. A. Jansen, "Modelling the influence of human behaviour on the spread of infectious diseases: a review," *J. R. Soc. Interface*, vol. 7, no. 50, pp. 1247–1256, 2010.
- [21] F. Verelst, L. Willem, and P. Beutels, "Behavioural change models for infectious disease transmission: a systematic review (2010–2015)," *J. R. Soc. Interface*, vol. 13, no. 125, p. 20160820, 2016.
- [22] N. Perra, D. Balcan, B. Gonçalves, and A. Vespignani, "Towards a characterization of behavior-disease models," *PLOS One*, vol. 6, no. 8, p. e23084, 2011.
- [23] C. Granell, S. Gómez, and A. Arenas, "Dynamical interplay between awareness and epidemic spreading in multiplex networks," *Phys. Rev. Lett.*, vol. 111, no. 12, p. 128701, 2013.
- [24] F. D. Sahneh, F. N. Chowdhury, and C. M. Scoglio, "On the existence of a threshold for preventive behavioral responses to suppress epidemic spreading," *Sci. Rep.*, vol. 2, no. 1, p. 632, 2012.
- [25] A. Rizzo, M. Frasca, and M. Porfiri, "Effect of individual behavior on epidemic spreading in activity driven networks," *Phys. Rev. E*, vol. 90, 2014.
- [26] K. Frieswijk, L. Zino, and M. Cao, "A time-varying network model for sexually transmitted infections accounting for behavior and control actions," *Int. J. Robust Nonlinear Control*, vol. 33, no. 9, pp. 4784–4807, 2023.
- [27] B. She, J. Liu, S. Sundaram, and P. E. Paré, "On a networked SIS epidemic model with cooperative and antagonistic opinion dynamics," *IEEE Trans. Control Netw. Syst.*, vol. 9, no. 3, pp. 1154–1165, 2022.
- [28] A. R. Hota and S. Sundaram, "Game-theoretic vaccination against networked SIS epidemics and impacts of human decision-making," *IEEE Trans. Control Netw. Syst.*, vol. 6, no. 4, pp. 1461–1472, 2019.
- [29] A. R. Hota, T. Sneh, and K. Gupta, "Impacts of game-theoretic activation on epidemic spread over dynamical networks," *SIAM J. Control Optim.*, vol. 60, no. 2, pp. S92–S118, Dec. 2021.
- [30] M. Ye, L. Zino, A. Rizzo, and M. Cao, "Game-theoretic modeling of collective decision making during epidemics," *Phys. Rev. E*, vol. 104, no. 2, p. 024314, 2021.
- [31] K. Frieswijk, L. Zino, M. Ye, A. Rizzo, and M. Cao, "A mean-field analysis of a network behavioral–epidemic model," *IEEE Control Syst. Lett.*, vol. 6, pp. 2533–2538, 2022.
- [32] K. Paarporp and C. Eksin, "SIS epidemics coupled with evolutionary social distancing dynamics," in *2023 Am. Control Conf.*, 2023, pp. 4308–4313.
- [33] A. Satapathi, N. K. Dhar, A. R. Hota, and V. Srivastava, "Coupled evolutionary behavioral and disease dynamics under reinfection risk," *IEEE Trans. Control Netw. Syst.*, vol. 11, no. 2, p. 795–807, 2024.
- [34] J. Certório, N. C. Martins, and R. J. La, "Epidemic population games with nonnegligible disease death rate," *IEEE Control Syst. Lett.*, vol. 6, pp. 3229–3234, 2022.
- [35] N. C. Martins, J. Certório, and R. J. La, "Epidemic population games and evolutionary dynamics," *Automatica*, vol. 153, p. 111016, 2023.
- [36] W. H. Sandholm, *Population games and evolutionary dynamics*. Cambridge MA, US: MIT Press, 2010.
- [37] P.-Y. Geoffard and T. Philipson, "Rational epidemics and their public control," *Int. Econ. Rev.*, vol. 37, no. 3, p. 603, Aug. 1996.
- [38] A. Ahituv, V. J. Hotz, and T. Philipson, "The responsiveness of the demand for condoms to the local prevalence of aids," *Journal of Human Resources*, pp. 869–897, 1996.
- [39] BBC News, "France makes condoms free for 18 to 25 year olds," <https://www.bbc.com/news/world-europe-63915467>, 2022, accessed: Oct 2024.
- [40] Centers for Disease Control and Prevention, "STD Awareness Week," <https://www.cdc.gov/std/saw/index.htm>, 2024, accessed: Oct 2024.
- [41] L. S. Pontryagin, *Mathematical theory of optimal processes*. Boca Raton FL, US: CRC Press, 1987.
- [42] S. Lenhart and J. T. Workman, *Optimal control applied to biological models*, 1st ed. New York NY, US: Chapman and Hall/CRC, 2007.

- [43] G. Como, F. Fagnani, and L. Zino, "Imitation dynamics in population games on community networks," *IEEE Trans. Control Netw. Syst.*, vol. 8, no. 1, pp. 65–76, 2021.
- [44] T. Philipson, "Private vaccination and public health: An empirical examination for U.S. measles," *J. Hum. Resour.*, vol. 31, no. 3, p. 611, 1996.
- [45] F. Blanchini, "Set invariance in control," *Automatica*, vol. 35, no. 11, pp. 1747–1767, 1999.
- [46] J. Guckenheimer and P. Holmes, *Nonlinear oscillations, dynamical systems, and bifurcations of vector fields*. New York NY, US: Springer, 2013.
- [47] O. Sharomi and T. Malik, "Optimal control in epidemiology," *Ann. Oper. Res.*, vol. 251, no. 1–2, p. 55–71, Mar. 2015.
- [48] L. Boyer, V. Pauly, Y. Brousse, V. Orleans, B. Tran, D. K. Yon, P. Auquier, G. Fond, and A. Duclos, "The impact of hospital saturation on non-covid-19 hospital mortality during the pandemic in france: a national population-based cohort study," *BMC Public Health*, vol. 24, no. 1, Jul. 2024.
- [49] J. W. Mold, R. M. Hamm, and L. H. McCarthy, "The law of diminishing returns in clinical medicine: How much risk reduction is enough?" *J. Am. Board Fam. Med.*, vol. 23, no. 3, p. 371–375, May 2010.
- [50] M. Pagone, M. Boggio, C. Novara, and S. Vidano, "A Pontryagin-based NMPC approach for autonomous rendez-vous proximity operations," in *2021 IEEE Aerospace Conf.*, 2021.
- [51] L. Warner and K. M. Stone, "Male condoms," in *Behavioral Interventions for Prevention and Control of Sexually Transmitted Diseases*. Springer, 2007, pp. 232–247.
- [52] J. E. Anderson, R. Wilson, L. Doll, T. S. Jones, and P. Barker, "Condom use and HIV risk behaviors among US adults: Data from a national survey," *Fam. Plan. Perspect.*, pp. 24–28, 1999.
- [53] M. Reece, D. Herbenick, V. Schick, S. A. Sanders, B. Dodge, and J. D. Fortenberry, "Condom use rates in a national probability sample of males and females ages 14 to 94 in the United States," *J. Sex. Med.*, vol. 7, pp. 266–276, 2010.
- [54] K. M. Kreisel, E. J. Weston, S. B. S. Cyr, and I. H. Spicknall, "Estimates of the prevalence and incidence of chlamydia and gonorrhea among us men and women, 2018," *Sex. Transm. Dis.*, vol. 48, no. 4, pp. 222–231, 2021.
- [55] J. A. Yorke, H. W. Hethcote, and A. Nold, "Dynamics and control of the transmission of gonorrhea," *Sex. Transm. Dis.*, vol. 5, no. 2, 1978.
- [56] G. A. Forster and C. A. Gilligan, "Optimizing the control of disease infestations at the landscape scale," *Proc. Natl. Acad. Sci. USA*, vol. 104, no. 12, pp. 4984–4989, 2007.
- [57] R. Morton and K. H. Wickwire, "On the optimal control of a deterministic epidemic," *Adv. in Appl. Probab.*, vol. 6, no. 4, pp. 622–635, 1974.
- [58] H. Behncke, "Optimal control of deterministic epidemics," *Optimal Control Appl. Methods*, vol. 21, no. 6, pp. 269–285, 2000.
- [59] D. C. Gesink, A. B. Sullivan, W. C. Miller, and K. T. Bernstein, "Sexually transmitted disease core theory: roles of person, place, and time," *Am. J. Epidemiol.*, vol. 174, no. 1, pp. 81–89, 2011.
- [60] H. L. Smith, *Monotone Dynamical Systems: An Introduction to the Theory of Competitive and Cooperative Systems*, 1st ed. Providence RI, US: American Mathematical Society, 1995.
- [61] G. Giordano et al., "Modelling the COVID-19 epidemic and implementation of population-wide interventions in Italy," *Nat. Med.*, vol. 26, pp. 855–860, 2020.
- [62] A. Rizzo, B. Pedalino, and M. Porfiri, "A network model for ebola spreading," *J. Theor. Biol.*, vol. 394, pp. 212–222, 2016.



FRANCESCO PARINO is a member of the EPIcx Lab, INSERM, Sorbonne Université, since November 2022. After getting his Master's Degree in Physics of Complex Systems at the University of Turin in 2017, Francesco Parino joined ISI Foundation for two years, working on big-data and machine-learning-related projects. In November 2019, he started his PhD at Politecnico di Torino, where he focused on the study of dynamic processes over complex networks, and the design

and optimal control of epidemiological models. He obtained his PhD (with honors) in June 2023. His interest concerns the development of epidemiology models that include mobility networks, the policy of interventions and individual behavior responses.



LORENZO ZINO (Senior Member, IEEE) is an Assistant Professor with the Department of Electronics and Telecommunications, Politecnico di Torino, Italy, since 2022. He received BS (2012), MS (summa cum laude, 2014), and PhD (with honors, 2018) in Applied Mathematics from Politecnico di Torino. He held Research Fellowships at Politecnico di Torino, University of Groningen, and New York University Tandon School of Engineering. His research interests include modeling, analysis, and control of dynamics over networks, applied probability, and game theory. He has co-authored more than 70 international scientific publications, including more than 40 journal papers. In 2024, he was the recipient of the Best Young Author Journal Paper Award from the IEEE CSS Italy Chapter. He is Associate Editor of the *Journal of Computational Science*, and member of the CEB for IEEE CSS and EUCA.



ALESSANDRO RIZZO (Senior Member, IEEE) received the Laurea degree (summa cum laude) in computer engineering and the PhD degree in automation and electronics engineering from the University of Catania, Italy, in 1996 and 2000, respectively. In 1998, he worked as a EURATOM Research Fellow with JET Joint Undertaking, Abingdon, UK, researching on sensor validation and fault diagnosis for nuclear fusion experiments. In 2000-01, he has worked as a Research Consultant at ST Microelectronics, Catania Site, Italy, and as an Industry Professor of robotics with the University of Messina, Italy. From 2002 to 2015, he was a tenured Assistant Professor with the Politecnico di Bari, Italy. Since 2012, he has been a Visiting Professor with the New York University Tandon School of Engineering, Brooklyn NY, US. In 2015, he joined Politecnico di Torino, where he is an Associate Professor in the DET and established the Complex Systems Laboratory. Dr. Rizzo is engaged in conducting and supervising research on cooperative robotics, complex networks and systems, modeling and control of nonlinear systems. He is the author of two books, two international patents, and about 200 papers on international journals and conference proceedings. He has been a recipient of the Award for the Best Application Paper at the IFAC WC in 2002 and of the Award for the Most Read Papers in Mathematics and Computers in Simulation (Elsevier) in 2009. He has also been a Distinguished Lecturer of the IEEE Nuclear and Plasma Science Society and one of the recipients of the 2019 and 2021 Amazon Research Awards in robotics.